ACS OMEGA

http://pubs.acs.org/journal/acsodf

Article

Test Strip Platform Spin-Off for Telomerase Activity Detection: Development of an Electrochemical Biosensor

Ramonita Díaz-Ayala,* Marjorie López-Nieves, Etienne S. Colón Berlingeri, Carlos R. Cabrera, Lisandro Cunci, Carlos I. González, and Pedro F. Escobar

Cite This: *ACS Omega* 2022, 7, 9964−9972

Read Online

ACCESS | Metrics & More | Article Recommendations | Supporting Information

ABSTRACT: Telomerase overexpression has been associated directly with cancer, and the enzyme itself is recognized within the scientific community as a cancer biomarker. BIDEA's biosensing strip (BBS) is an innovative technology capable of detecting the presence of telomerase activity (TA) using electrochemical impedance spectroscopy (EIS). This BBS is an interdigital gold (GID) electrode array similar in size and handling to a portable glucose sensor. For the detection of the biomarker, BBS was modified by the immobilization of a telomere-like single strand DNA (ssDNA) on its surface. The sensor was exposed to telomerase-positive extract from commercially available cancer cells, and the EIS spectra were measured. Telomerase recognizes the sequence of this immobilized ssDNA probe on the BBS, and the reverse transcription process that occurs in cancer cells is replicated, resulting in the ssDNA probe elongation. This surface process caused by the presence of TA generates changes in the capacitive process on the electrode array microchip surface, which is followed by EIS as the sensing tool and correlated with the presence of cancer cells. The telomerases' total cell extraction protocol results demonstrate significant changes in the charge-transfer resistance (R_{ct}) change rate after exposure to telomerase-positive extract with a detection limit of 2.94×10^4 cells/mL. Finally, a preliminary study with a small set of "blind" uterine biopsy samples suggests the feasibility of using the changes in the R_{ct} magnitude change rate $(\Delta(\Delta R_{ct}/R_{cti})/\Delta t)$ to distinguish positive from negative endometrial adenocarcinoma samples by the presence or absence of TA.

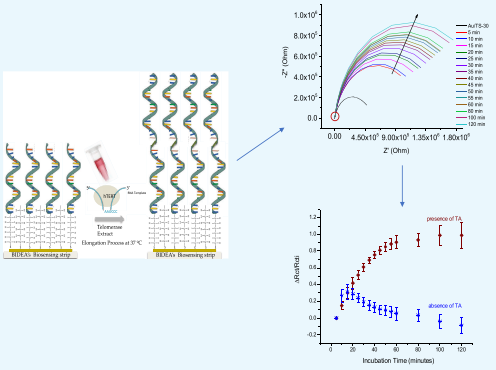

INTRODUCTION

Uterine cancer (UC) is the fourth[1] most common invasive cancer of the female reproductive system. Starting in the endometrium, the internal lining of the uterus begins to grow out of control, and if not detected or treated early, it can spread to other areas of the body, decreasing the survival chance and success of treatment, as well as increasing costs.[2,3] While women over 50 years old are the group that exhibits the major probabilities to suffer UC (90% of incidence), four percentage of women diagnosed with this type of cancer are younger than 40 and remain fertile.[4] The incidence and mortality of endometrial cancer (EC) has been increasing through the years. Although most EC does not run-in families, about 5% is inherited. For example, a woman who suffers Lynch syndrome has a much higher chance (15−60%) of developing colorectal and endometrial (uterine) cancer.[5,6] Taking into consideration all these facts, it is clear how important and imminent it is to have routine tests for EC. There is an urgent need to screen for EC at its early stages before the clinical signs and symptoms arrive and the cancer spreads; a test that helps doctors differentiate between cancer and normal tissue is key.[7] Currently, there is no standard or routine screening test for EC other than pathology tests that may take at least 1 or 2 weeks to receive the full report. The screening method evaluated in this study presents an opportunity to offer early treatment and decrease morbidity and mortality rates.

Telomerase is a ribonucleoprotein complex that contains both an RNA fragment that catalyzes the addition of TTAGGG repeats on the telomeric end of the chromosomal DNA and a reverse transcriptase component,[8,9] identified by its enzymatic activity in 1985 by Elizabeth Blackburn and Carol Greider.[10]

Soon after its discovery, Gregg Morin in 1989 identified telomerase activity (TA) in human cells, while in 1994, Counter et al.[11] linked its reactivation with cancer cell proliferation.[10] Therefore, telomerase has been shown to be overexpressed in most different types of malignant tumors, making it a useful biomarker for cancer diagnosis.[12−14]

Received: February 3, 2022
Accepted: February 17, 2022
Published: March 9, 2022

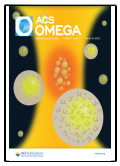

Telomerase is an enzyme whose activities are essential for cellular immortality, and it is observed in almost 90% of malignant cells,[14,15] including EC cells.[16−19] Telomerase has been reported as an epithelial cancer cell biomarker,[20] which can be used in early cancer detection, prognosis, and/or subsequent monitoring of residual cancer. Because telomerase is absent in most normal somatic cells, telomerase activity (TA) detection is an excellent cancer biomarker. Despite these important facts, the number of publications initially was limited because of difficulties involved in detecting TA. It was not until the development of the telomeric repeat amplification protocol (TRAP),[21,22] a polymerase chain reaction (PCR)-based assay increased the ability to detect TA; a more significant number of telomerase-related manuscripts began. However, this method is time-consuming, expensive, requires specialized instruments, among some other drawbacks.

The scientific literature regarding telomerase detection methods is currently a proliferative area and seems promising. Some claim incredible detection limits[23−29] and proposed very novel processes.[29,30] However, some of them involve complex procedures,[23] others with a relative complexity of the output signal (i.e., SERS methods),[24,27] the use of sophisticated instruments that will represent a challenge when translating from the laboratory bench to the physician's office as a tool for detection, diagnosis, and monitoring cancer. Others do not report results with complex samples, such as biological samples (tissues samples).[24,26,28−30] Despite all reported prospective developing methods, TRAP continues to be the standard-of-gold method for telomerase detection. However, its use is only for research and does not represent an alternative screening or diagnostic. Our research group (BIDEA) offers a powerful and innovative technology with a high potential of becoming a screening test for the early detection of uterine/EC cells. This was demonstrated via trials, and the feasibility of this technology of becoming a routine test for women is promising. BIDEA's technology can detect the presence of TA using electrochemical impedance spectroscopy (EIS) analysis. The use of EIS as a detection method in biosensors has been an extremely active field of study for several reasons. EIS has high sensitivity, with minimal hardware requirements as well as its possibilities of scalability and miniaturization.[31,32] All these characteristics give EIS the advantage of being a manufacturable and portable medical device, such as those currently in the market, glucometers.

In this article, BIDEA successfully demonstrates how our gold (Au) interdigitated (GID) electrode array or BIDEA's biosensor strip (BBS), which was modified by the immobilization of telomere-like ssDNA on its surface, showed changes in the charge-transfer resistance (R_{ct}) process when it is exposed to extract from cancer cells. The technology proposed takes advantage of the telomerase and its ssRNA template by tethering a telomere-like ssDNA biomolecule probe. Then, the telomerase bonds and elongates the probe, blocking electronic and capacitive processes on the microelectrode surface. This change is detected by measuring the impedance using EIS and correlated to the activity of telomerase, which indicates the presence of cancer cells. Although, a lot of work has been reported using telomerase as a cancer biomarker and other biosensors employing EIS as the detection method, a very reduced number of studies couple both.[33−35] The innovation of this work consists in developing a biosensing test strip that allows for the detection of TA via EIS in a quick form, and the impedance measurement, using EIS, makes it compatible with many portable electronic devices.

In this work, we successfully demonstrated the feasibility of our sensing technology to detect the existence of EC cells via the detection of TA by measuring sensitive electrochemical events occurring at the interface of our sensor strip surface using EIS. This is coupled with the specificity provided by exclusive biomolecules only present in cancer cells combining the use of EIS, which accurately measures specific electrochemical interactions with a GID, a system of only two electrodes, and without the need of sensitive enzymes anchored to the electrode's surface. DNA probes are easily synthesized and tethered to the GID electrode to be more robust and less expensive than enzymes. The results demonstrate that changes in R_{ct} can be used to distinguish positive from negative endometrial adenocarcinoma samples by detecting the presence or absence of TA.

EXPERIMENTAL SECTION

Cell Culture and Extraction Methods. Commercial human uterine adenocarcinoma cancer cell line HEC-1-A (ATCC HTB-112) was obtained from the American Type Culture Collection (ATCC, Manassas, VA). HEC-1-A cells are cancer cells that use the telomerase enzyme in their process of becoming immortal,[36] and telomerase is the target of our biosensor; thus, HEC-1-A represents a positive control. To grow and subculture the HEC-1-A cell line, we followed the manufacturer's protocol[37] and detailed it in the Supporting Information.

Telomerase extract preparation was accomplished through the following steps:[38] (1) cells were collected in the exponential phase of growth, and 1×10^6 cells/mL were washed twice with ice-cold phosphate-buffered saline (PBS) 1× (140 mM NaCl, 2.7 M KCl, 10 mM $NaHPO_4$, and 1.8 mM KH_2PO_4). (2) Then, cells were resuspended in ice-cold 3-[3-(cholamidopropyl)dimethylammonio]-1-propanesulfonate (CHAPS) lysis buffer [10 mM Tris−HCl, pH 7.5, 1 mM $MgCl_2$, 1 mM ethylenediaminetetraacetic acid (EDTA), 0.1 mM phenylmethanesulfonyl fluoride (PMSF), 0.5% CHAPS, 10% glycerol] with a final concentration of 25×10^6 cells/mL. (3) The suspension was then incubated for 30 min on ice and centrifuged for 20 min at 15,000 rpm, 4 °C. (4) Finally, the supernatant was carefully transferred to a fresh tube and frozen at −80 °C until use.

Extract Preparation from Uterine Biopsy Samples. For the extract preparation from the real sample, 50−80 mg of frozen tissue was used. First, it was washed in cold wash buffer [10 mM 4-(2-hydroxyethyl)-1-piperazineethanesulfonic acid (HEPES)-KOH at pH-7.5, 1.5 mM $MgCl_2$, 10 mM KCl, 1 mM dithiothreitol (DTT)] to remove possible contaminants and blood from the surface of the sample and then resuspended in 200 μL of ice-cold 1X CHAPS lysis buffer in a sterile 1.5 mL microcentrifuge tube. The sample was homogenized with a mechanical homogenizer until uniform consistency. The homogenization cycle consisted of intervals of 10 s homogenizing and 30 s resting in ice for approximately 5 min. The sample was kept on ice during homogenization to prevent heat accumulation. Then, it was incubated on ice for 30 min, and the sample was spinned in a microcentrifuge at 15,000 rpm for 20 min at 4 °C. The supernatant (telomerase extract) was transferred into a fresh tube in small-volume aliquots, quick-frozen on dry ice, and stored at −80 °C. The total protein concentration was determined using the Bradford

https://doi.org/10.1021/acsomega.2c00713
ACS Omega 2022, 7, 9964−9972

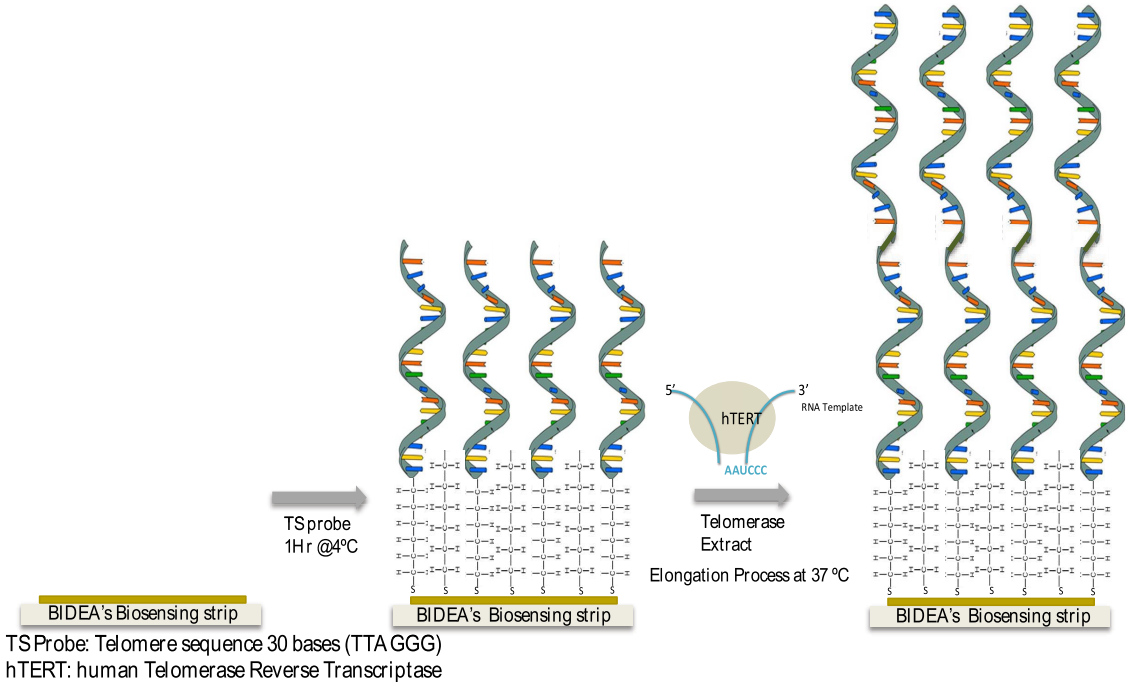

Figure 1. Schematic representation for the tethering of the TS-30 probes on the GID electrode and the elongation mechanism responsible for the change in the impedance during incubation at 37 °C.

assay. *All the experiments were done in compliance with the Federalwide Assurance (FWA) for the Protection of Human Subjects: (FWA #: FWA00029431). Written informed consent was obtained from the patients for sample collection, and external IRB (Advarra IRB: IRB00000971) was approved for the protocol (Pro00031039).*

Biosensor Microchip Construction and Characterization. *Telomerase Substrate Immobilization.* Commercially available Au interdigital electrode strips were used as a biosensor platform. These electrodes were modified with single-strand DNA (ssDNA) probes for telomerase sensing. A characteristic voltammogram for a clean gold electrode was obtained, as shown in Figure S1.

Prior to the immobilization of the 1 μM telomerase substrate (TS-30) (Sequence: 5′HO-$(CH_2)_6$-S-S-$(CH_2)_6$TTTTTTTTTTAATCCGTCGAGCAGAGTT-3′) onto the gold-sensing strip surface, TS-30 was dissolved in immobilization buffer (I-buffer: 10 mM Tris−HCl, 0.1 M NaCl, 10 μM TCEP at pH 7.5) and incubated for 30 min at room temperature to reduce the disulfide bonds.[39] After the activation of the thiol group, 10 μL of TS-30 solution was placed on the cleaned sensing strip for 1 h of immobilization at 4 °C. Afterward, the sensing strips were washed carefully with nanopure water, 0.05% sodium dodecyl sulfate (SDS) for 1 min, and then dried with N_2 flux. Nanopure water was previously treated with diethylpyrocarbonate (DEPC) and autoclaved to inactivate RNase and DNase enzymes.

Electrochemical Characterization. For electrochemical experiments, a digital potentiostat/galvanostat PGSTAT 204/FRA 32 M (Metrohm Autolab B.V., Utrecht, UT, The Netherlands) controlled with Nova only driver 2.1.3 software was employed. First, the sensing strip was electrochemically cleaned by cycling between a potential range from 0 to 1.5 V vs Ag/AgCl (3 M NaCl) in 0.5 M sulfuric acid solution at 300, 200, and 100 mV/s scan rates until a reproducible voltammogram was obtained. Then, the sensing strips modified with TS-30 were characterized electrochemically by cyclic voltammetry (CV), as well as EIS, using telomerase extract coming from HEC-1-A. Figure 1 shows each step of the BBS construction.

CV was recorded following the redox behavior of 2 mM $K_3Fe(CN)_6/K_4Fe(CN)_6$ solution in the PBS buffer from 0.3 to −0.3 V vs OCP (open-circuit potential) at a scan rate of 50 mV/s. EIS experiments were conducted from 1.0 MHz to 0.1 Hz, taking 40 measurements in the logarithmic scale, with an amplitude of 10 mV, single sine method at 0.000 V vs OCP. The solution containing the biomarker under study comes from commercial samples. These samples were placed in 2.0 mL microtubes in a thermomixer at 37 °C, and the impedance was measured by EIS every 5 min during the first 60 min, followed by three additional measurements every 20 min.

RESULTS AND DISCUSSION

BBS Construction and Characterization. The modification of the GID electrode was electrochemically characterized by CV and EIS at every step of the modification process to assure the quality of sensor fabrication; see Figure S2. A decrease in the redox current response was observed, as well as a small shift toward higher oxidation and reduction potential after the GID electrode was modified with TS-30 was observed (see Figure S2a). These electrochemical changes are attributed to the insulating effect of the ssDNA on the Au surface. Its immobilization interferes and limits the free electron transfer between the redox couple in solution and the GID electrode surface. Equally, the electrode exhibited a significant change in impedance, confirming the deposition of the TS-30 on the surface, as seen in Figure S2b. Because impedance is a measure of resistance occurring on the electrode surface, the Nyquist plots in Figure S2b showed that the impedance for the GID electrode modified with TS-30 increased compared to the bare and clean GID electrode. The electrochemical response changes observed in the CV and the EIS plots confirmed the immobilization of TS-30 on the GID surface. Linear sweep

https://doi.org/10.1021/acsomega.2c00713
ACS Omega 2022, 7, 9964−9972

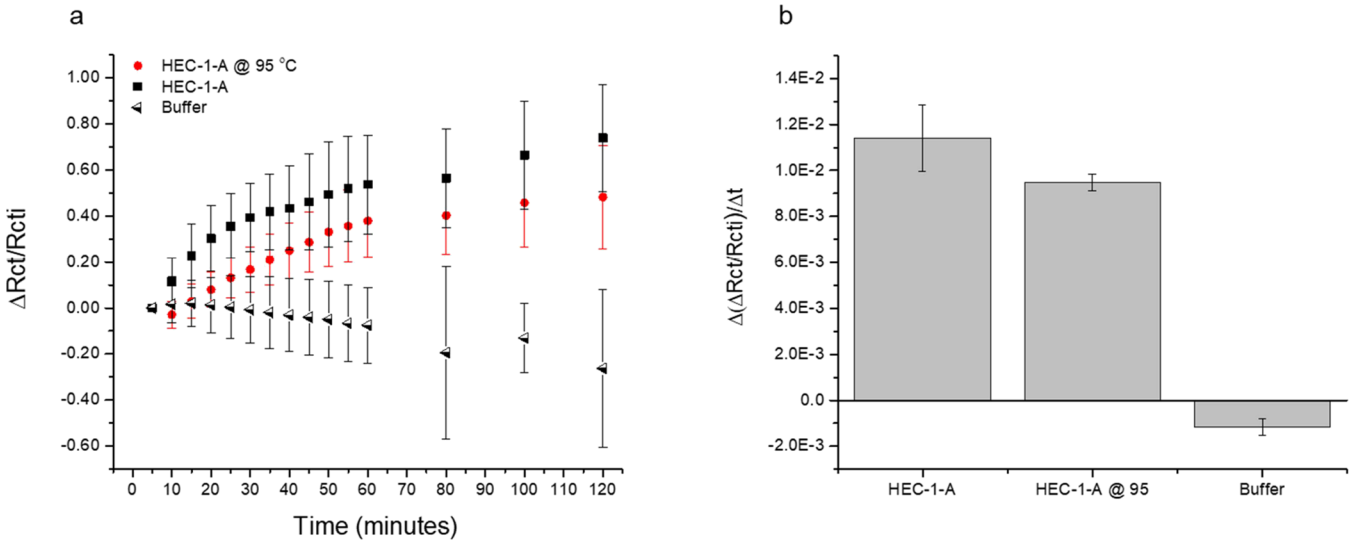

Figure 2. (a) Variation in charge-transfer resistance ($\Delta R_{ct}/R_{cti}$) in the function of incubation time for different controls (1×10^6 cells/mL) (solid square) EC cell line (HEC-1-A), (red circle) preheated HEC-1-A at 95 °C, (triangle) buffer, (b) relative change in resistance to charge transfer to telomerase reaction time for different concentrations (positive and negative controls). Error bars represent the standard deviations of 4 to 5 parallel replicates.

voltammetry (LSV) shown in Figure S3 gives a better characterization and understanding of the modified surface. Two peaks were observed in the LSV, indicating the immobilization of more than one species of the GID electrode surface.

The presence of these two desorption peaks is indispensable to understand the TS-30 structure. TS-30 is an alkanethiol composed of a head thiol group (−SH) that binds to the gold surface through a strong covalent-like bond (Au−S), an alkyl spacer chain $(CH_2)_6$, and a tail group. Commercial TS comes with its thiol group in an oxidized form, with the sulfur atoms protected by an S−S bond, while the tail groups of both sides of the S atoms contain different spacer chains. In one of them, the 30-base oligonucleotide TS-30 is present, while the other sulfur has an hexanol group. For this reason, a reduction step to activate the thiol group of the TS-30 before the immobilization process was used. The reduction mechanism generates two molecules available for the immobilization at the GID surface: (1) the ssDNA-thiolate (TS-30 or HS-$(CH_2)_6$TTTTTTTTTTAATCCGTCGAGCAGAG TT) and (2) a hydroxyalkylthiolate, better known as mercaptohexanol (MCH or HO−$(CH_2)_6$−SH), as shown in Figure S4. Indeed, the immobilization of thiol-TS-30 on the GID surface was conducted via the formation of a self-assembled monolayer (SAM). Regarding this fact, we expect our TS-30 SAM to be a mixed monolayer having TS-30 and MCH-thiolates in accordance with the presence of two electrodesorption peaks in the LSV. Furthermore, a TS-30 surface density of (4.9×10^{-10} mol/cm^2) for TS-30 SAM (1 h) was determined by integrating the area of the desorption peak obtained by LSV, while for MCH at 1 h of immobilization, the surface density was 8.8×10^{-10} mol/cm^2.

Electrochemical Response with Biological Samples. The modified GID electrodes were incubated in the cell extract where the telomerase was present. The elongation reaction of the ssDNA (TS-30), generated by the presence of telomerase in cell extracts, was evaluated by EIS, as shown in Figure S5. The Nyquist plot in Figure S5a represents the real impedance (Z') versus the imaginary impedance ($-Z'$) for a GID electrode modified with TS-30 for 1 h and exposed to telomerase extract. The spectrum of impedance allowed us to characterize the surface of the GID to detect the activity of telomerase based on the magnitude of the impedance of the electrode. To achieve this analysis and to be able to interpret the complex value of the impedance spectrum (Nyquist plot), the plot was fitted to an equivalent circuit. One of the most frequently cited equivalent circuits that fitted EIS spectra is the Randles equivalent circuit.[40] In this work, the exhibited Nyquist plots are fitted by an adapted Randles equivalent circuit, where the ideal capacitor is replaced by a constant-phase element (CPE).[31,41] Figure S5b represents the solution resistance (R_s), charge-transfer resistance (R_{ct}), and double-layer capacitance (C_{dl}). Thus, extrapolating the semicircle to the Z_{real} axis, we were able to determine the R_{ct} and how this changed with incubation time (GID electrode in the telomerase extract) or cancer cell concentration. It should be noted in Figure S5a that the amplitude of impedance increases gradually with time as the repeated units of TTAGGG are continually added to the 3′ end of the TS-30. In general, the impedance measurement from curves of 5 up to 120 min becomes larger, which is attributed to the number of repeat units being added. The elongation process of TS-30 was described by a slightly deformed semicircle because of the surface layer, and consequently, the ion layer at the surface is not completely homogeneous.

Calibration Curve, Positive and Negative Controls. To establish the feasibility of our proposal, EIS was evaluated with three control samples such as (a) the telomerase extract from HEC-1-A as the positive control, (b) preheated telomerase extract at 95 °C to turn telomerase inactive (negative control) and (b) buffer medium as blank. Using the same concentrations (1×10^6 cells/mL) for all control samples and a modified GID electrode with TS-30 for 1 h, EIS studies were performed. The changes in R_{ct} were related to the elongation process of TS-30 by TA. The results in Figure 2 show a small decrement in R_{ct} variations for those samples identified as a negative control: preheated telomerase extract from HEC-1-A, and remarkably different with the blank, both

https://doi.org/10.1021/acsomega.2c00713
ACS Omega 2022, 7, 9964−9972

Table 1. Sample Concentration and TRAP RT Telomerase Detection Results

sample	cells/mL	protein concentration (Bradford assay) (∞g/mL)	C_t (threshold cycle)	copy number (telomerase activity)	C_t samples heated at 95 °C	copy number (telomerase activity)
HEC-1-A (May 7)	5.0×10^6	1405.98	29.80	3.518×10^5	41.55	1.094×10^3
HEC-1-A (May 14)	25.0×10^6	1624.64	28.95	5.352×10^5	38.54	4.795×10^3
no telomerase control (buffer)	N/A	N/A	38.22	5.621×10^3		

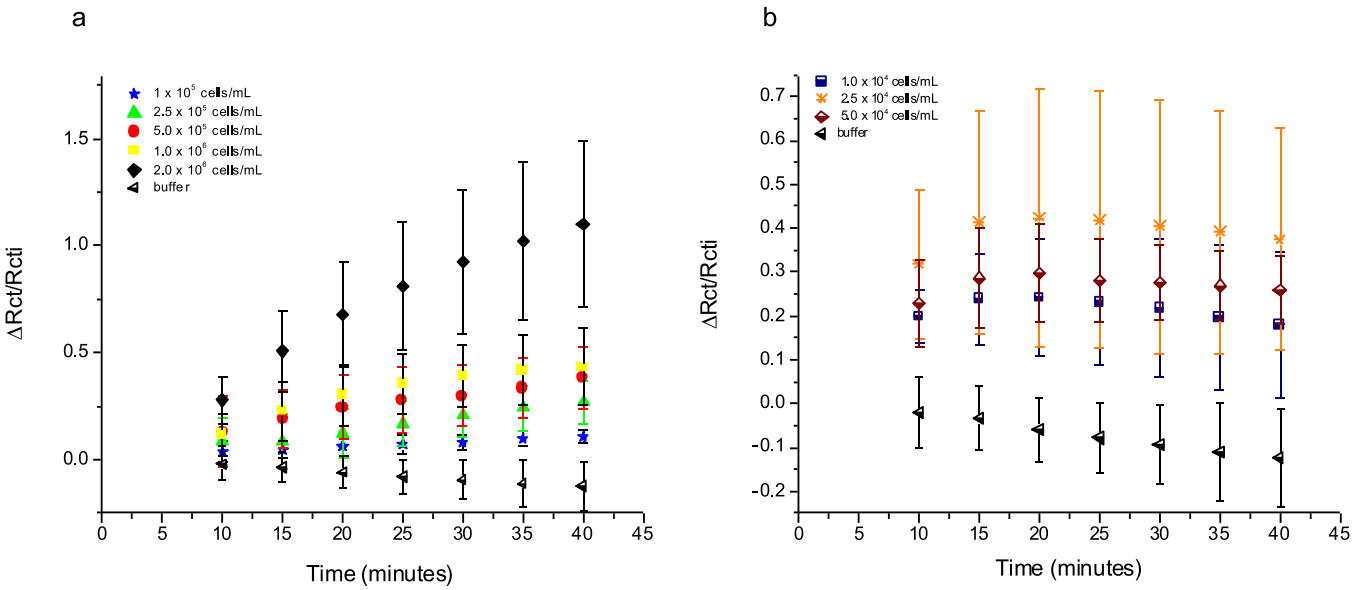

Figure 3. Charge-transfer resistance change ($\Delta R_{ct}/R_{cti}$) of BBS for TA as a function of incubation time. Sensitivity of BBS for TA detection. The measurements were taken with different concentrations of telomerase extracted from (a) 1.0×10^5, 2.5×10^5, 5×10^5, 1.0×10^6, and 2.0×10^6 HEC-1-A cells/mL and (b) 1×10^4, 2.5×10^4, and 5.0×10^4 cells/mL. Extraction buffer represents a 0 cells/mL concentration. Error bars represent the standard deviations of five to six parallel replicates.

cases in comparison with the positive control. The more noticeable difference in impedance, positive control vs blank, is attributed to the TS-30 extension process caused by the presence or absence of TA. The cases with minor changes in R_{ct} result from a low TA, that is, preheated telomerase extract. The apparent prevalence of TA in the negative control could be attributed to an inefficient inhibition process. Preheating the sample for 10 min at 95 °C would not be enough to denature all telomerase present in the sample and inactivate it. It is crucial to distinguish the results shown in Figure 2a, b and their respective standard deviation error bars. Figure 2a shows replicates (n = 5) for each control, and the relative significant error bars show how accurate the mean value represents the individual data. This means a high dispersion between each data point and the mean. It does not indicate that the data are invalid but points out that factors like the BBS and sample preparation need improvement. In experiments that involve biological events, measurements are notoriously variable. However, Figure 2a shows that our technology's sensitivity is good, and differences for each control are significant.

These results are comparable with those obtained with other research laboratory techniques such as the TRAPeze RT telomerase kit, which was used to validate our results. This PCR based on the telomerase-extended product detection method allows for identifying and quantifying TA by directly measuring real-time fluorescence emission in the reaction vessel. Furthermore, the threshold cycle (C_t) was used as an indicator of the DNA elongation process because of the repeat telomeric sequences added by TA. C_t is the cycle threshold, or the number of PCR cycles required to obtain a fluorescence signal.[42] For example, real-time PCR results for those samples with high TA will exhibit a higher DNA copy number compared to those with smaller DNA copy numbers (see Table 1). It is notable how the TA in the positive control, HEC-1-A, showed decay after it was heat-treated. This happens because telomerase is a heat-sensitive enzyme, and it becomes inactivated when it is incubated for 10 min at 95 °C. Heat destroys the essential RNA template and the reverse transcriptase protein of telomerase. TRAP results exhibited the behavior that we anticipate and explain with our EIS method for samples coming from different batches: telomerase extraction from different batches, despite using the same extraction protocol and cells/mL concentration; results are not necessarily equal regarding the total protein concentration and TA. Simultaneously, the differences exhibited for the buffer (in which the telomerase extract was substituted for the lysis buffer) and attributed to TA absence compared to the positive control are more evident in both methods (experimental using EIS and TRAP), as shown by Ct in Table 1.

The C_t values are for positive controls with values between 29 and 30. All of them were heated, and they exhibited a C_t displacement toward C_t values greater than or equal to that exhibited by the buffer (no telomerase control), C_t = 39. This displacement toward higher C_t values occurred in the heated samples, where TA's inactivation is expected. The fluorescence emission produced is directly proportional to the number of

https://doi.org/10.1021/acsomega.2c00713
ACS Omega 2022, 7, 9964−9972

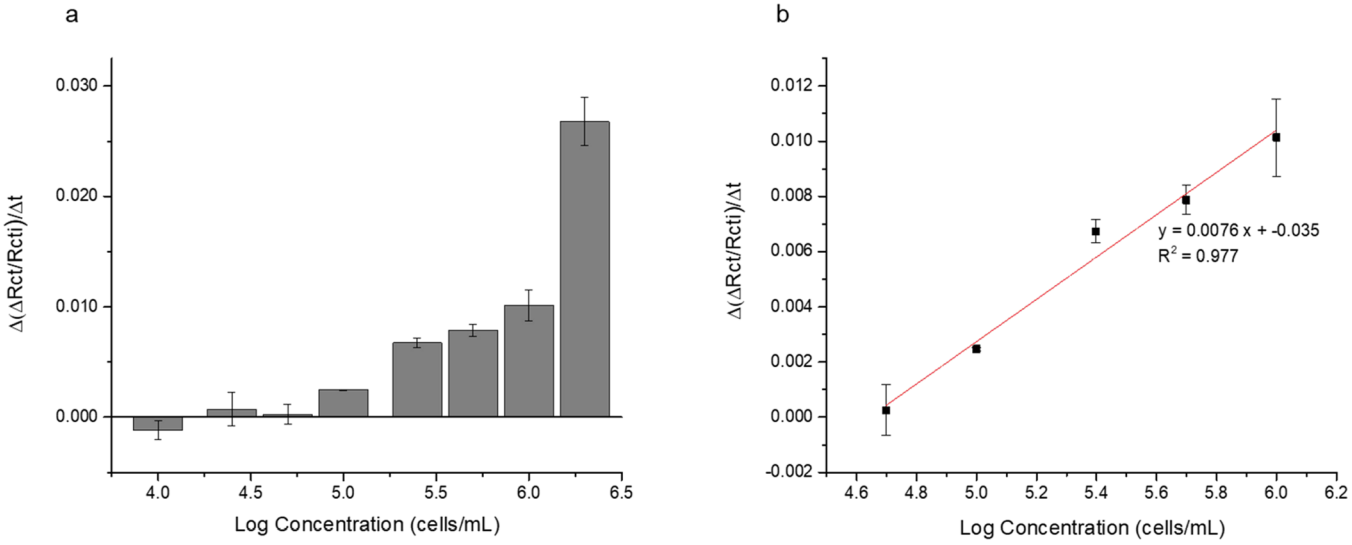

Figure 4. (a) Comparison of the R_{ct} magnitude change rate $(\Delta(\Delta R_{ct}/R_{cti})/\Delta t)$ vs cancer cell concentrations in cells/mL of the BBS for TA. The measurements were taken at different whole-cell extract concentrations, 1.0×10^5, 2.5×10^5, 5×10^5, 1.0×10^6, and 2.0×10^6 HEC-1-A cells/mL. (b) Linear relationship between $(\Delta(\Delta R_{ct}/R_{cti})/\Delta t)$ and the logarithm of cell extract concentrations.

TRAP products (telomerase substrate), extended products generated. A comparison with the blank of the generated copy number in both control positive and negative allows discriminating between the direct result of the PCR reaction and TA. These results not only show the feasibility of our platform to detect telomerase but also suggests that it is analogous with the TRAPeze assays, providing an extraordinary sensitivity. The next objective is to establish parameters, such as sensitivity and detection limits.

Once demonstrated the viability to distinguish between the positive and negative samples and determine the GID biosensor's sensitivity, the relationship between cancer cell concentrations in cells/mL and the R_{ct} magnitude change rate $(\Delta(\Delta R_{ct}/R_{cti})/\Delta t)$ was investigated. A range of eight concentrations was analyzed (see Figure 3a, b). R_{ct} changes for different concentrations and at specific times were evaluated. A positive response is observed in a concentration range of 2.0×10^6 cell/mL to 2.5×10^4 cells/mL, and then, a negative response occurred at 1×10^4 cells/mL. The response in this graph was obtained during the first 40 min of the EIS measurements. This behavior suggests that additional studies should be performed at concentrations below this value (1×10^4 cells/mL), which have match boundaries between cancerous and noncancerous samples. As shown in Figure 2a and observed in Figure 3a, b, the difference in charge-transfer resistance between buffer and samples of different cells/mL concentrations is significant. Nevertheless, a high standard deviation (error bars) could be observed, especially in samples with telomerase extract coming from a lower cell/mL concentration. As discussed before, it suggests how minor differences in BBS modification, sample preparation, or replicating the measurement could be significantly affected by the measurement, especially when the TA is small. In contrast, an evaluation of the sensitivity (the graph slope) of the BBS response, R_{ct} magnitude change rate $(\Delta(\Delta R_{ct}/R_{cti})/\Delta t)$ vs cancer cell concentrations, exhibited small standard deviation error bars. This suggested a significant difference in $(\Delta(\Delta R_{ct}/R_{cti})/\Delta t)$ that allows for discrimination between samples with different TAs.

The elongation process occurs by the addition of several telomeric repeats (TTAGGG) at the 3′ end of TS-30; thus, at higher concentrations of telomerase, the number of telomeric repeats increases in comparison to low telomerase concentration. This fact is evident in the EIS biosensing experimental results. Figure 4a shows a remarkable R_{ct} change rate at different concentrations, and a major sensitivity is observed at higher concentrations up to 1×10^5 cells/mL. A strong linear correlation was observed between the logarithmic concentration and the R_{ct} magnitude change rate. The linear equation was attained from the linear relation $(y = 0.0076x + -0.035)$, where (y) is R_{ct} magnitude change rate $(\Delta(R_{ct}/R_{cti})/\Delta t)$, and (x) represents the logarithm of different concentrations of HEC-1-A. (Figure 4b) Using the standard methods for determining the limit of blank (LoB) and the limit of detection (LoD) published by Clinical and Laboratory Standards Institutes (CLSI), the detection limit was calculated.[43,44] From eq 1, the LoB, the highest value expecting to be observed from a sample that contains no analyte (buffer), was determined to be $(-1.11 \times 10^{-3}\ \Omega/\text{min})$. Then, substituting the LoB value in eq 2, the signal corresponding to the "lowest" analyte concentration likely to be reliably distinguished from the LoB and at which detection is "feasible" was obtained.

$$\text{LoB} = \text{mean}_{\text{Blank}} + 1.645(\text{sd}_{\text{Blank}}) \quad (1)$$

$$\text{LoD} = \text{LoB} + 1.645(\text{sd}_{\text{low concentration sample}}) \quad (2)$$

Using the LoD values and the linear equation for the relationship between the R_{ct} magnitude change rate and the logarithmic of concentration HEC-1-A, the detection limit was calculated to be 2.94×10^4 cells/mL. This value is under the findings shown in Figure 3b. At concentrations below 5.0×10^4 cells/mL, we could observe a sensitivity decrease and a random behavior with enormous error bars. However, these variabilities open the doors to more studies to improve this LoD. While the preliminary results obtained with uterine biopsy samples and discussed below placed this biosensor in that frontier of being capable of spotting the earliest detectable precancerous perturbations, more studies are needed in this area before establishing a conclusion.

https://doi.org/10.1021/acsomega.2c00713
ACS Omega 2022, 7, 9964−9972

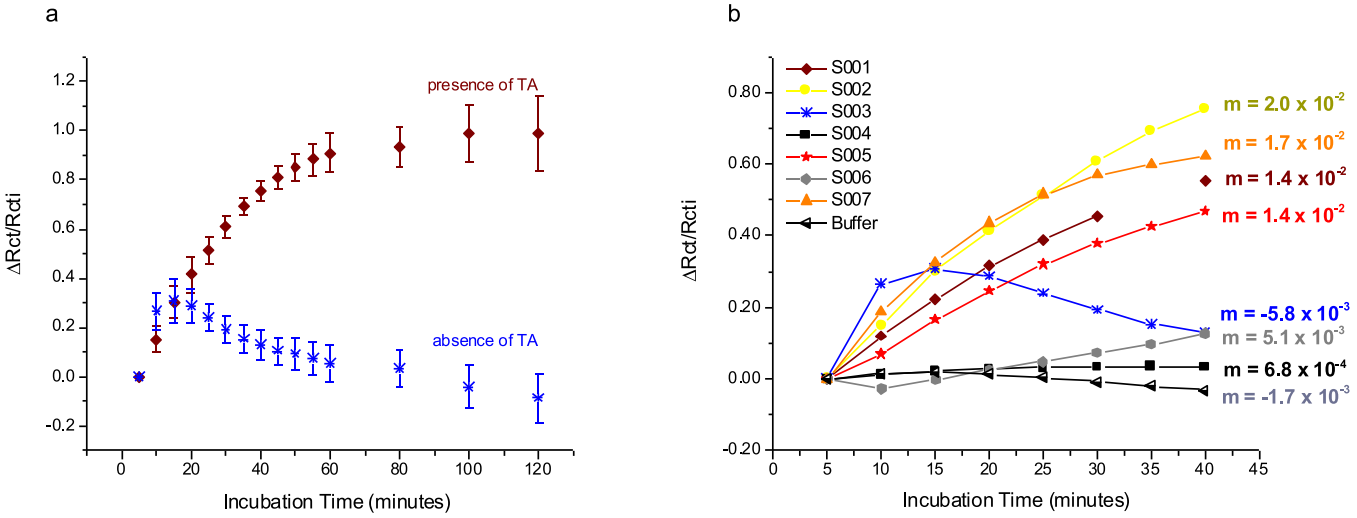

Figure 5. (a) EIS for R_{ct} change ($\Delta R_{ct}/R_{cti}$) measurements as a function of incubation time in the (◆) presence and (∗) absence of telomerase activity. (b) Variation in charge-transfer resistance (R_{ct}) in function of incubation time for different endometrial biopsy samples and the buffer.

Table 2. Results for Endometrial Biopsy Samples Using Diagnostic Pathology versus BBS[a]

sample	pathologic diagnosis	reported by literature telomerase activity (TA)	reference	TRAP results	our results ($(\Delta R_{ct}/R_{cti})/\Delta t$)
S00l	endometrial hyperplasia with atypia	exhibited TA	46	TA activity	positive $m = 1.4 \times 10^{-2}$
S002	no endometrial tissue seen/abundant mucoid material	no expected TA		TA activity	positive $m = 2.0 \times 10^{-2}$
S003	negative for malignancy. Acute and chronic inflammation with bacteria colonies	no expected TA		no TA activity	negative $m = -5.8 \times 10^{-3}$
S004l	atrophic endometrium (AE). Leiomyomas, intramural.	AE may exhibit low TA	46		negative (o below LoD) $m = 6.8 \times 10^{-4}$
S005	low-grade squamous intraepithelial lesion, focal. Proliferative endometrium (PE) myometrium unremarkable	may exhibit TA	46		positive $m = 1.4 \times 10^{-3}$
S006	fragments of atrophic endometrium. immunohistochemical: P-16 negative, Kl-67 negative, P-53 negative	no expected TA		No TA activity	negative (or below LoD) $m = 5.1 \times 10^{-3}$
S007	congenital adrenal hyperplasia (CAH)	unknown		TA activity	positive $m = 1.7 \times 10^{-2}$

[a]Ref 46.

Pilot Study with Uterine Biopsy Samples. Seven double-blinded endometrial biopsies were evaluated with the BBS. The diagnosis of samples, positive or negative, was unknown to BIDEA and to the gynecologist−oncologist (Gyn-Onc). The Gyn-Onc provided a fraction of the endometrial biopsy, the other fraction was sent for diagnostic pathology, and then, both results were compared. BIDEA only processed samples from those patients who received a biopsy prescription and consented for a fraction of their samples to be used in this study. The samples were evaluated by BIDEA's innovative proposed biosensing methodology and corroborated with the TRAP assay. Two convincing examples, in which the presence of TA (Sample 002) and lack of TA (Sample 003) are suggested, are shown in Figure 5a. Both samples exemplify dramatically different behaviors in R_{ct} changes with respect to time. However, when we evaluate the slope of the variation in R_{ct} during the incubation time for each sample during the first 40 min and compare them with the standard samples, we can suggest a TA result (either positive or negative). The value of the signal for the LoB determined with the equation of the LOD (eq 2) results in a R_{ct} magnitude change rate ($\Delta(R_{ct}/R_{cti})/\Delta t$) (slope of the curve) of -1.1×10^{-3} Ω/min that suggested that those samples with a negative slope in the graph of ($\Delta R_{ct}/R_{cti}$) vs time are negative, Figure 5b. Those with a slope near zero will be negative samples or under our detection limits. In contrast, samples with a positive slope in the graph of ($\Delta R_{ct}/R_{cti}$) vs time are positive (Samples 001, 002, 005, and 007). These results, although validated by the TRAP assay, are not in agreement with the diagnostic pathology (Table 2). The diagnostic pathology is a qualitative assay, while BIDEA results are quantitative TA measurements.

Although the diagnostic pathology results were negative for all the samples analyzed in this study, the diagnosed conditions may exhibit TA because they are considered precancerous lesions, as previously reported.[45] Although this study analyzed a small number of cases with uncertainty that varies from 20 to 40%, it represents a suitable proof-of-concept that requires additional testing.

Therefore, BBS can potentially become a routine screening tool and play a pivotal role in reducing the incidence and mortality rates of EC. This biomedical sensing technology is particularly novel and unique not only because it allows for

https://doi.org/10.1021/acsomega.2c00713
ACS Omega 2022, 7, 9964−9972

rapid cancer cell detection but also because the impedance measurement, using EIS, makes it potentially compatible with many portable electronic devices. This interaction, between a molecular biology event and an electrochemical microchip response, qualifies as a selective and sensitive in vitro diagnostic device (IVD) that no other biomedical device can deliver.

CONCLUSIONS

This work demonstrates that our BBS and EIS technique results in a reliable way to detect TA. Our outcomes are in accordance with the commonly used methods, such as the TRAP assay. The results validate the total cell extraction protocol as an appropriate one.

This BBS showed to effectively detect the presence or absence of TA in real-time in complex samples as obtained through whole-cell lysis and with detection limits of 2.94×10^4 cells/mL. EIS results show maximum impedimetric changes within the first 15 to 40 min. Also, the magnitude in R_{ct} changes will provide a good idea about the presence or absence of TA and could be used to discriminate between different cancer stages. These findings suggest that reliable results can be obtained quickly and that EIS will be used as a quantitative method for screening TA.

Future work includes the validation and fine-tuning of this technology with many known positive and negative endometrial biopsy samples. This will enable us to obtain a deeper understanding of the sensing process with real tissues, which will, in turn, allow us to establish tendencies and to optimize EIS parameters with endometrial samples from a biopsy.

ASSOCIATED CONTENT

Supporting Information

The Supporting Information is available free of charge at https://pubs.acs.org/doi/10.1021/acsomega.2c00713.

Details of the preparation of cell culture and extraction methods, detailed description of the BBS construction characterization, figures, and references (PDF)

AUTHOR INFORMATION

Corresponding Author

Ramonita Díaz-Ayala − *BIDEA LLC, Molecular Science Research Center, San Juan 002926-2614, Puerto Rico;* orcid.org/0000-0001-8131-7058; Email: ramonita.diaz@upr.edu

Authors

Marjorie López-Nieves − *BIDEA LLC, Molecular Science Research Center, San Juan 002926-2614, Puerto Rico*

Etienne S. Colón Berlingeri − *BIDEA LLC, Molecular Science Research Center, San Juan 002926-2614, Puerto Rico*

Carlos R. Cabrera − *BIDEA LLC, Molecular Science Research Center, San Juan 002926-2614, Puerto Rico; Department of Chemistry and Biochemistry, University of Texas at El Paso, El Paso, Texas 79968, United States*

Lisandro Cunci − *BIDEA LLC, Molecular Science Research Center, San Juan 002926-2614, Puerto Rico; School of Natural Sciences and Technology, Universidad Ana G. Méndez, Puerto Rico 00778, United States;* orcid.org/0000-0002-7315-177X

Carlos I. González − *BIDEA LLC, Molecular Science Research Center, San Juan 002926-2614, Puerto Rico; Department of Biology, University of Puerto Rico, San Juan 00931-3346, Puerto Rico*

Pedro F. Escobar − *Department of Obstetrics and Gynecology, Division of Gynecologic Oncology, University of Puerto Rico, School of Medicine, San Juan 00926, Puerto Rico*

Complete contact information is available at: https://pubs.acs.org/10.1021/acsomega.2c00713

Notes

The authors declare no competing financial interest.

ACKNOWLEDGMENTS

This project was supported in part by Small Business Innovation Research (SBIR) Phase I grant from the National Science Foundation (NSF-IIP Grant No. 1746384) and the Puerto Rico Science, Technology & Research Trust (Grant No. 2018-00074). We are most grateful to Dr. Nadja E. Solís-Marcano, Sherly A. Nieves-Cruz, and Alexis Acevedo-González for critical reading of this manuscript.

REFERENCES

(1) Adishesh, M.; Fyson, A.; DeCruze, S. B.; Kirwan, J.; Consortium, E.; Werner, H. M. J.; Hapangama, D. K. Harmonisation of biobanking standards in endometrial cancer research. *Br. J. Cancer* **2017**, *117*, 485−493.

(2) Brand, A.; Dubuc-Lissoir, J.; Ehlen, T. *Diagnosis of endometrial cancer in women with abnormal vaginal bleeding*; 2000.

(3) SGO Clinical Practice Endometrial Cancer Working Group; Burke, W. M.; Orr, J.; Leitao, M.; Salom, E.; Gehrig, P.; Olawaiye, A. B.; Brewer, M.; Boruta, D.; Herzog, T. J.; Shahin, F. A.; Society of Gynecologic Oncology Clinical Practice Committee. Endometrial cancer: a review and current management strategies: part II. *Gynecol. Oncol.* **2014**, *134*, 393−402.

(4) Colombo, N.; Creutzberg, C.; Amant, F.; Bosse, T.; Gonzalez-Martin, A.; Ledermann, J.; Marth, C.; Nout, R.; Querleu, D.; Mirza, M. R.; Sessa, C.; ESMO-ESGO-ESTRO Endometrial Consensus Conference Working Group. ESMO-ESGO-ESTRO Consensus Conference on Endometrial Cancer: diagnosis, treatment and follow-up. *Ann. Oncol.* **2016**, *27*, 16−41.

(5) Meyer, L. A.; Broaddus, R. R.; Lu, K. H. Endometrial cancer and Lynch syndrome: clinical and pathologic considerations. *Cancer Control* **2009**, *16*, 14−22.

(6) Wang, Y.; Wang, Y.; Li, J.; Cragun, J.; Hatch, K.; Chambers, S. K.; Zheng, W. Lynch syndrome related endometrial cancer: clinical significance beyond the endometrium. *J. Hematol. Oncol.* **2013**, *6*, 22.

(7) Pertynski, T.; Wozniak, K.; Romanowicz-Makowska, H.; Czechowska, A.; Blasiak, J. Telomerase expression and activity endometrial cancer. *Exp. Oncol.* **2002**, *24*, 5.

(8) Yi, Z.; Wang, H. B.; Chen, K.; Gao, Q.; Tang, H.; Yu, R. Q.; Chu, X. A novel electrochemical biosensor for sensitive detection of telomerase activity based on structure-switching DNA. *Biosens. Bioelectron.* **2014**, *53*, 310−315.

(9) Zhao, Y.; Abreu, E.; Kim, J.; Stadler, G.; Eskiocak, U.; Terns, M. P.; Terns, R. M.; Shay, J. W.; Wright, W. E. Processive and distributive extension of human telomeres by telomerase under homeostatic and nonequilibrium conditions. *Mol. Cell* **2011**, *42*, 297−307.

(10) Corey, D. R. Telomeres and Telomerase: From Discovery to Clinical Trials. *Chem. Biol.* **2009**, *16*, 1219−1223.

(11) Counter, C. M.; Hirte, H. W.; Bacchetti, S.; Harley, C. B. Telomerase activity in human ovarian carcinoma. *Proc. Natl. Acad. Sci. U. S. A.* **1994**, *91*, 2900−2904.

(12) Shay, J. W.; Wright, W. E. Senescence and immortalization: role of telomeres and telomerase. *Carcinogenesis* **2005**, *26*, 867−874.

(13) Shay, J. W.; Wright, W. E. Telomerase: a target for cancer therapeutics. *Cancer Cell* **2002**, *2*, 257−265.

(14) Kyo, S.; Inoue, M. Complex regulatory mechanisms of telomerase activity in normal and cancer cells: how can we apply them for cancer therapy? *Oncogene* **2002**, *21*, 688−697.
(15) Shay, J. W.; Zou, Y.; Hiyama, E.; Wright, W. E. Telomerase and cancer. *Hum. Mol. Genet.* **2001**, *10*, 677−685.
(16) Kyo, S.; Kanaya, T.; Takakura, M.; Tanaka, M.; Inoue, M. Human telomerase reverse transcriptase as a critical determinant of telomerase activity in normal and malignant endometrial tissues. *Int. J. Cancer* **1999**, *80*, 60−63.
(17) Kyo, S.; Kanaya, T.; Ishikawa, H.; Ueno, H.; Inoue, M. Telomerase activity in gynecological tumors. *Clin. Cancer Res.* **1996**, *2*, 2023−2028.
(18) Kyo, S.; Takakura, M.; Kohama, T.; Inoue, M. Telomerase activity in human endometrium. *Cancer Res.* **1997**, *57*, 610−614.
(19) Oshita, T.; Nagai, N.; Ohama, K. Expression of telomerase reverse transcriptase mRNA and its quantitative analysis in human endometrial cancer. *Int. J. Oncol.* **2000**, *17*, 1225−1230.
(20) Gauthier, L. R.; Granotier, C.; Soria, J. C.; Faivre, S.; Boige, V.; Raymond, E.; Boussin, F. D. Detection of circulating carcinoma cells by telomerase activity. *Br. J. Cancer* **2001**, *84*, 631−635.
(21) Kim, N. W.; Piatyszek, M. A.; Prowse, K. R.; Harley, C. B.; West, M. D.; Ho, P. L.; Coviello, G. M.; Wright, W. E.; Weinrich, S. L.; Shay, J. W. Specific association of human telomerase activity with immortal cells and cancer. *Science* **1994**, *266*, 2011−2015.
(22) Gilson, E.; Segal-Bendirdjian, E. The telomere story or the triumph of an open-minded research. *Biochimie* **2010**, *92*, 321−326.
(23) Liu, Y.; Li, S.; Zhang, L.; Zhao, Q.; Li, N.; Wu, Y. Catalytic Hairpin Assembly-Assisted Rolling Circle Amplification for High-Sensitive Telomerase Activity Detection. *ACS Omega* **2020**, *5*, 11836−11841.
(24) Guo, X.; Wu, X.; Sun, M.; Xu, L.; Kuang, H.; Xu, C. Tetrahedron Probes for Ultrasensitive In Situ Detection of Telomerase and Surface Glycoprotein Activity in Living Cells. *Anal. Chem.* **2020**, *92*, 2310−2315.
(25) Eom, G.; Kim, H.; Hwang, A.; Son, H.-Y.; Choi, Y.; Moon, J.; Kim, D.; Lee, M.; Lim, E.-K.; Jeong, J.; Huh, Y.-M.; Seo, M.-K.; Kang, T.; Kim, B. Nanogap-Rich Au Nanowire SERS Sensor for Ultra-sensitive Telomerase Activity Detection: Application to Gastric and Breast Cancer Tissues Diagnosis. *Adv. Funct. Mater.* **2017**, *27*, No. 1701832.
(26) Mahmoudi, T.; Pirpour Tazehkand, A.; Pourhassan-Moghaddam, M.; Alizadeh-Ghodsi, M.; Ding, L.; Baradaran, B.; Razavi Bazaz, S.; Jin, D.; Ebrahimi Warkiani, M. PCR-free paper-based nanobiosensing platform for visual detection of telomerase activity via gold enhancement. *Microchem. J.* **2020**, *154*, No. 104594.
(27) Yang, G.; Zhang, Q.; Ma, L.; Zheng, Y.; Tian, F.; Li, H.; Zhang, P.; Qu, L.-L. Sensitive detection of telomerase activity in cells using a DNA-based fluorescence resonance energy transfer nanoprobe. *Anal. Chim. Acta* **2020**, *1098*, 133−139.
(28) Sun, L.; Zhao, Q.; Liu, X.; Pan, Y.; Gao, Y.; Yang, J.; Wang, Y.; Song, Y. Enzyme-mimicking accelerated signal enhancement for visually multiplexed quantitation of telomerase activity. *Chem. Commun.* **2020**, *56*, 6969−6972.
(29) Meng, F.; Chen, X.; Cheng, W.; Hu, W.; Tang, Y.; Miao, P. Ratiometric Electrochemical Sensing Strategy for the Ultrasensitive Detection of Telomerase Activity. *ChemElectroChem* **2019**, *6*, 2000−2003.
(30) Liu, X.; Meng, F.; Sun, R.; Wang, K.; Yu, Z.; Miao, P. Three-dimensional bipedal DNA walker enabled logic gates responding to telomerase and miRNA. *Chem. Commun.* **2021**, *57*, 2629−2632.
(31) Santos, A.; Davis, J. J.; Bueno, P. R. Fundamentals and Applications of Impedimetric and Redox Capacitive Biosensors. *J. Anal. Bional. Tech.* **2014**, *S7*, 15.
(32) Hammond, J. L.; Formisano, N.; Estrela, P.; Carrara, S.; Tkac, J. Electrochemical biosensors and nanobiosensors. *Essays Biochem.* **2016**, *60*, 69−80.
(33) Cunci, L.; Vargas, M. M.; Cunci, R.; Gomez-Moreno, R.; Perez, I.; Baerga-Ortiz, A.; Gonzalez, C. I.; Cabrera, C. R. Real-Time Detection of Telomerase Activity in Cancer Cells using a Label-Free Electrochemical Impedimetric Biosensing Microchip. *RSC Adv.* **2014**, *4*, 52357−52365.
(34) Diaz-Cartagena, D. C.; Hernández-Cancel, G.; Bracho-Rincon, D. P.; González-Feliciano, J. A.; Cunci, L.; Gonzalez, C. I.; Cabrera, C. R. Development of an electrochemical impedimetric biosensor for the detection of Telomerase activity in cancer cells. *ECS Trans.* **2017**, *77*, 8.
(35) Yang, W.; Zhu, X.; Liu, Q.; Lin, Z.; Qiu, B.; Chen, G. Label-free detection of telomerase activity in HeLa cells using electrochemical impedance spectroscopy. *Chem. Commun.* **2011**, *47*, 3129−3131.
(36) Murakami, J.; Nagai, N.; Shigemasa, K.; Ohama, K. Inhibition of telomerase activity and cell proliferation by a reverse transcriptase inhibitor in gynaecological cancer cell lines. *Eur. J. Cancer* **1999**, *35*, 1027−1034.
(37) Delivered, T. E. O. L. S. R. G. HEC-1-A Cell Line Protocol. http://www.atcc.org/products/all/HTB-112.aspx.
(38) Zhang, L.; Zhang, S.; Pan, W.; Liang, Q.; Song, X. Exonuclease I manipulating primer-modified gold nanoparticles for colorimetric telomerase activity assay. *Biosens. Bioelectron.* **2016**, *77*, 144−148.
(39) IDT (I.D.T.) Reduction Protocol for Thiol-Modified Oligonucleotides. https://sfvideo.blob.core.windows.net/sitefinity/docs/default-source/protocol/reduction-protocol-for-thiol-modified-oligonucleotides.pdf?sfvrsn=431c3407_6 (accessed August 29, 2019).
(40) Radhakrishnan, R.; Suni, I. I.; Bever, C. S.; Hammock, B. D. Impedance Biosensors: Applications to Sustainability and Remaining Technical Challenges. *ACS Sustainable Chem. Eng.* **2014**, *2*, 1649−1655.
(41) Pilehvar, S.; Dierckx, T.; Blust, R.; Breugelmans, T.; De Wael, K. An electrochemical impedimetric aptasensing platform for sensitive and selective detection of small molecules such as chloramphenicol. *Sensors* **2014**, *14*, 12059−12069.
(42) Yang, L.; Ellington, A. D. Real-time PCR detection of protein analytes with conformation-switching aptamers. *Anal. Biochem.* **2008**, *380*, 164−173.
(43) Armbruster, D. A.; Pry, T. Limit of blank, limit of detection and limit of quantitation. *Clin. Biochem. Rev.* **2008**, *29*, S49−S52.
(44) Little, T. A. Method Validation Essentials, Limit of Blank, Limit of Detection, and Limit of Quantitation. *BioPharm Int.* **2015**, *28*, 4.
(45) Alnafakh, R. A. A.; Adishesh, M.; Button, L.; Saretzki, G.; Hapangama, D. K. Telomerase and Telomeres in Endometrial Cancer. *Front. Oncol.* **2019**, *9*, 344.
(46) Chen, X. J.; Zheng, W.; Chen, L. L.; Chen, Z. B.; Wang, S. Q. Telomerase antisense inhibition and chemotherapeutic combination treatments for the proliferation of endometrial cancer in vitro and in vivo. *Chin. Med. J.* **2004**, *84*, 1721−1725.

https://doi.org/10.1021/acsomega.2c00713
ACS Omega 2022, 7, 9964−9972